Single- and multiple-electron effects in the Si 1s photoabsorption spectra of SiX_4 (X = H,D,F,Cl,Br,CH_3,C_2H_5,OCH_3,OC_2H_5) molecules: Experiment and theory

S. Bodeur
Laboratoire pour l'Utilisation du Rayonnement Electromagnétique, Université de Paris–Sud, 91405 Orsay CEDEX, France
and Laboratoire de Chimie Physique, 11 rue Pierre et Marie Curie, 75231 Paris CEDEX 05, France

P. Millié
Département d'Etude des Lasers et de Physico-Chimie, Centre d'Etudes Nucléaires de Saclay, 91191 Gif-sur-Yvette CEDEX, France

I. Nenner
Laboratoire pour l'Utilisation du Rayonnement Electromagnétique, Université de Paris–Sud, 91405 Orsay CEDEX, France
and Département d'Etude des Lasers et de Physico-Chimie, Centre d'Etudes Nucléaires de Saclay, 91191 Gif-sur-Yvette CEDEX, France
(Received 31 July 1989)

New or improved photoabsorption spectra of gas-phase silicon molecules SiX_4 (X = H,D,F,Cl,Br,CH_3,C_2H_5,OCH_3,OC_2H_5) have been measured near the silicon 1s edge in the 1830–1900-eV photon energy range. On the basis of configuration-interaction calculations performed on the core-equivalent species, we show that for SiH_4 and SiF_4 the two lowest resonances are due to excitation of the Si 1s electron into unoccupied orbitals, both having a mixed-valence Rydberg character. For all other systems, there is a unique intense transition into a pure low-lying valence orbital, and all Rydberg states have a negligible oscillator strength. Vibronic coupling effects are found in the intensity of a symmetry-forbidden valence transition, but only for X = F,Cl,Br. In addition, we interpret multiplet features found in the immediate vicinity above the ionization edge, as double core-valence vacancy-excited states. Possible overlap of such states with shape resonance in SiX_4 (X = F,OCH_3,OC_2H_5) is discussed.

I. INTRODUCTION

The detailed understanding of resonances observed in photoabsorption spectra of gas-phase molecules is of fundamental interest because they give important information on the electronic properties of the considered species in a well-defined geometrical arrangement. Therefore, they can be considered as model systems for understanding more complex systems in the condensed phase, for which such resonances (so-called XANES for x-ray-absorption near-edge structures) are commonly studied for the determination of the local order near an atomic site.

In a recent paper on photoabsorption spectra of some gas-phase silicon compounds[1] recorded near the silicon 1s edge, we have shown on a qualitative basis that the most pronounced resonances could be described using simple symmetry considerations for electric-dipole selection rules. In addition, we observed large differences in the discrete spectra of SiF_4 as compared to those of $SiCl_4$ [or $Si(CH_3)_4$]. We proposed, using the core-equivalent model, that a Jahn-Teller effect was responsible for the removal of the degeneracy of the most intense degenerate transition Si $1s \rightarrow \sigma(t_2)^*$, especially in the SiF_4 case. Meanwhile, Bozek *et al.*[2] reported high-resolution photoabsoprtion spectra of SiO_4 near the Si 2s and Si 2p edges. Very recently, Tse *et al.*[3] analyzed the available experimental data[1,2] using multiple-scattering $X\alpha$ calculations.

In the present paper, we have revisited our previous assignment using new experimental photoabsorption spectra in a larger series of silicon compounds molecules and new theoretical calculations. In particular, we report the following.

(i) We present photoabsorption spectra of tetrahedral molecules SiX_4 (H,D,F,Cl,Br,CH_3,OCH_3,C_2H_5,OC_2H_5) obtained near the silicon 1s edge, either reported for the first time or recorded at higher resolution than previously published work.[1,4]

(ii) We present *ab initio* configuration-interaction (CI) calculations on the core-equivalent species, in order to offer an assignment of valence and Rydberg states in SiX_4 (X=H,F,Cl,Br). We show that valence-Rydberg mixing, found only for X=H and F, explains the unusual intensity of the low-lying Rydberg transition. We also show that vibronic effects are responsible for symmetry-forbidden transitions.

(iii) We offer a new assignment of some narrow near-edge resonances in terms of double core-valence vacancy-excited states and discuss possible configuration-interaction mixing with shape resonances when fluorine or oxygen are the neighboring atoms of the silicon atom.

 ©1990 The American Physical Society

II. EXPERIMENT

A. Method

Photoabsorption spectra were obtained using synchrotron radiation from the ACO (Anneau de Collision d'Orsay) storage ring, with a double crystal monochromator[5] equipped with two InSb(111) crystals ($2d = 7.4806$ Å). This monochromator provides a photon beam with an intensity of the order of 10^5 photon/s in a 0.4-eV bandpass around 1850 eV. The monochromatic beam enters a gas cell. In the present work, we have used two different cells closed with polypropylene windows, one (143 mm long) for conventional photoabsorption measurements as described previously,[1,7,8] another (100 mm long) for ionization yield measurements. For conventional photoabsorption measurements, the detection of the transmitted x-ray beam is ensured by an ionization chamber filled with air at a pressure of 200 Torr. For ionization yield measurements, we used a gas pressure of about 0.5 Torr. An electrode positioned in the cell along the beam direction is polarized with respect to the body of the cell and is used to measure the total ionization yield signal. This method provides essentially the same results as the traditional photoabsorption technique.[7] Some differences of around 0.4 eV can be found in the width of narrow features and slight differences of a few tenths of an eV can be found in the energy of the structures.[1] However, the origin of those differences is not clear at this time.

The SiX_4 (X=Br,CH_3,OCH_3,C_2H_5,OC_2H_5) molecules, normally liquid at room temperature, are commercially available from the Fluka Company with a stated purity of 99.9%. They were used without further purification other than repeated freeze-pump thaw cycles to remove dissolved gases. SiF_4 and $SiCl_4$ gases are commercially available from the Prodair Company with a purity of 99.5% and 99.999%, respectively, and SiH_4 from the Air Liquid Company (99.9% purity). The deuterated silane has been obtained by the reduction of $SiCl_4$ with $LiAlD_4$.[9] They were introduced in the cell without further purification. As most of the gases under study are rapidly hydrolyzed by moist air, a passivation of the mounting (cell and valves) by repeated flushing cycles of $Si(CH_3)_3Cl$ was necessary to eliminate residual water vapor before admission of the gas. In the case of photoabsorption measurements, according to the gas under study, typical pressures, measured accurately with a capacitance manometer, were chosen between 1 and 10 Torr, in order to be sufficiently low to avoid absorption saturation[10] and yet sufficiently high to have a good contrast between the spectral features under study and the continuum.

Spectra were obtained by automatic scans of the photon energy in successive runs. For XANES spectra, we have chosen small steps (0.1 eV) in order to measure reliably all possible fine structures within the limit of the resolving power. Typical recording times of the absorption spectra amount to 15 to 30 min, depending on the extension of the wavelength range. The absorption spectra are extracted simply from $\ln(I_0/I)$ and put on a relative intensity scale. The photon energy scale was determined carefully from measured Bragg angles. The monochromator calibration is obtained according to the energy region studied by recording well-known spectra as reference systems. In the Si K region, we have used a Si-C:H solid sample for which the onset of K absorption occurs at (1836.7±0.1) eV.[11] We estimate the accuracy of the absolute energy scales better than 0.5 eV and the relative energies of sharp features within a single spectrum reproducible to better than 0.1 eV.

TABLE I. Experimental energies, term values, relative intensities, and suggested assignment of near-edge resonances in SiX_4 (X=H,D,F,Cl,Br). Values in parentheses denote the energies for SiD_4. IP refers to ionization potential.

Peak	Energies (eV)	E_{TV} (eV)	Assignment
	SiH_4 (SiD_4)		
1	1842.5 (1842.7)	4.5	t_2
2	1844.2 (1844.4)	2.8	$4p$
3	1845.8 (1854.8)	1.2	$5p$
IP	1847.0	0	
4 (shoulder)	1848.4 (1849.5)	−1.4	doubly excited
5	1852.9 (1853.2)	−5.9	doubly excited
6 (shoulder)	1854.5 (1854.7)	−7.5	doubly excited
7	1857.1 (1857.7)	−10.1	doubly excited
8 (shoulder)	1860.0 (1860.0)	−13.0	doubly excited
9 (shoulder)	1862.5 (1862.5)	−15.5	doubly excited
10 (shoulder)	1866.0 (1866.0)	−19.0	doubly excited
11	1924	−77.0	EXAFS
	SiF_4		
1	1846.5	6.0	a_1
2	1849.0	3.5	t_2
3	1850.2	2.3	$4p$
IP	1852.5	0	
4 (shoulder)	1858.0	−5.5	doubly excited shape
5	1865.0	−12.5	doubly excited shape
6	1934	−81.5	EXAFS
7	2058	−205.5	EXAFS
	$SiCl_4$		
1 (shoulder)	1844.8	5.8	a_1
2	1846.0	4.6	t_2
IP	1850.6	0	
3	1851.0	−0.4	doubly excited
4	1857.7	−7.1	doubly excited
5	1860.5	−9.9	doubly excited
6	1875.0	−24.4	shape
7	1918	−67.4	EXAFS
8	1998	−147.4	EXAFS
	$SiBr_4$		
1 (shoulder)	1843.0	6.7	a_1
2	1845.0	4.7	t_2
3	1849.5	0.2	doubly excited
IP	1849.7	0	
4 (shoulder)	1851.6	−1.9	doubly excited
5	1855.2	−5.5	doubly excited
6	1869.0	−19.3	shape
7	1916	−66.3	EXAFS

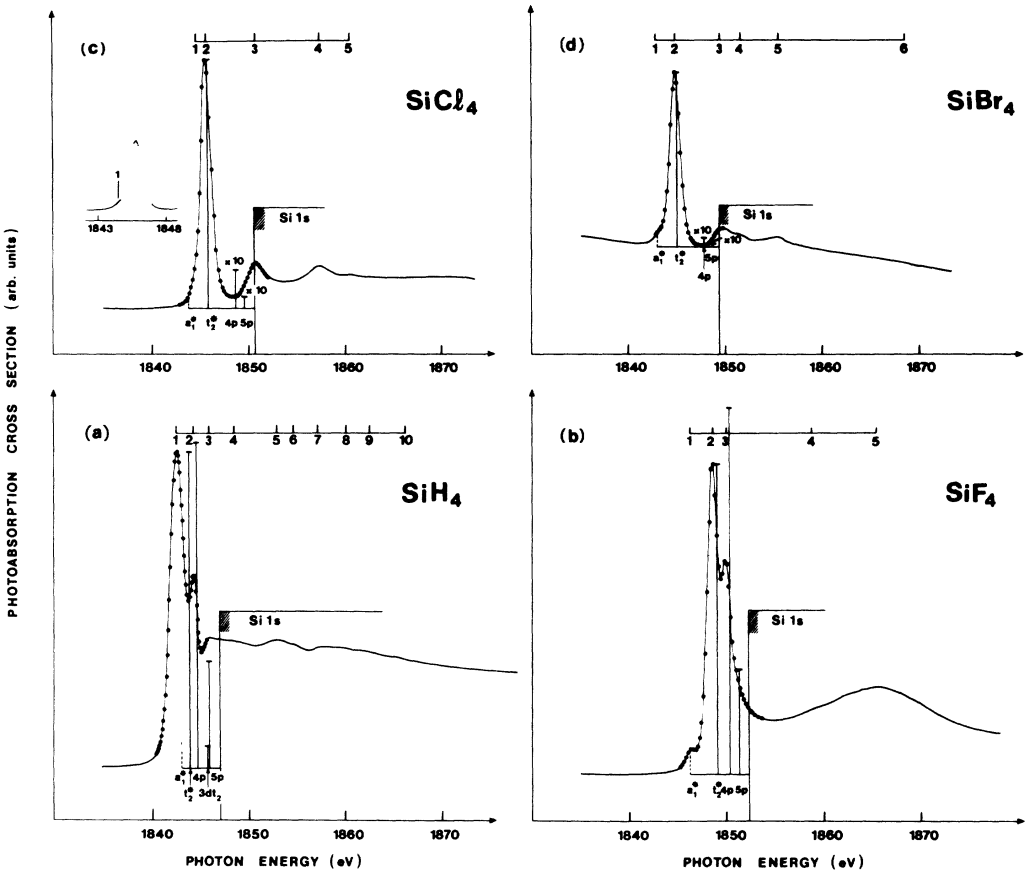

FIG. 1. Photoabsorption spectra of SiX_4 (X=H,F,Cl,Br) molecules between 1830 and 1880 eV photon energy. The vertical bars denote CI calculations on the core-equivalent molecules.

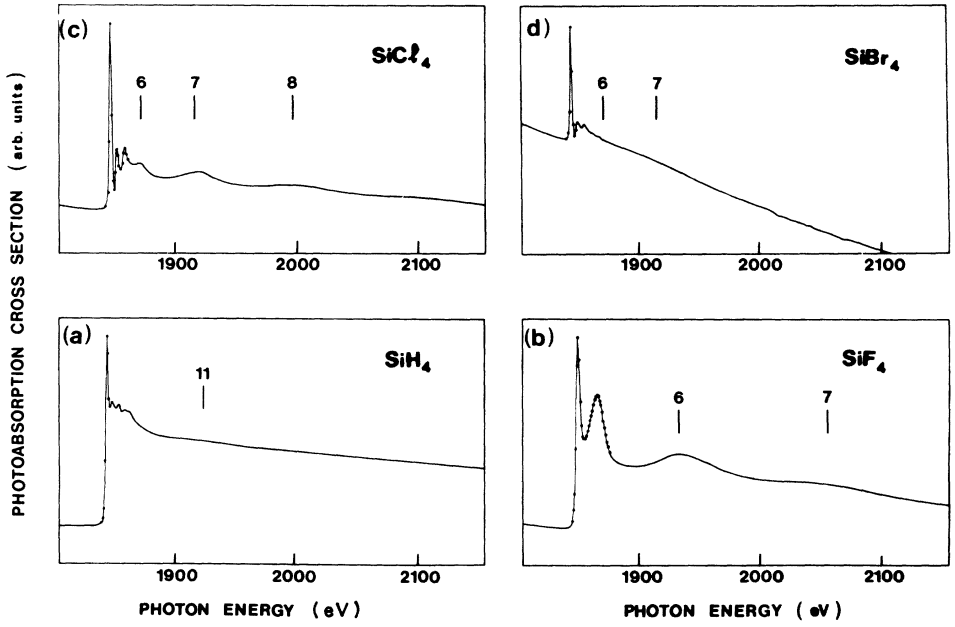

FIG. 2. Photoabsorption spectra of SiX_4 (X=H,F,Cl,Br) molecules between 1830 and 2150 eV photon energy.

B. Results

We present in Fig. 1, the photoabsorption spectra of SiX_4 (X=H,F,Cl,Br) in the 1830–1880-eV photon energy range. In Fig. 2, we show the same spectra in an extended photon energy range, i.e., 1800–2150 eV. This presentation is made to emphasize the presence of both very narrow and very wide resonances. The spectra of the hydrogenated, fluorinated, and chlorinated molecules are very close to our previous measurements,[1,4] except that the signal-to-noise and wavelength bandpass have been improved. For $SiCl_4$, the present Si 1s spectrum resembles the Si 2s one reported in Ref. 2, at least for the two lowest intense resonances. For the tetrabromide molecule the gross features of the spectrum have been shown recently.[12] The spectra presented in Fig. 1 show the region near the Si 1s edge, at high resolution. In order to evaluate term values for each resonance and allow a comparison with theory, we have indicated in Fig. 1 the energy of the silicon 1s ionization limit. This energy has been extracted either directly from photoelectron spectroscopy (for SiH_4, see Ref. 13) or indirectly from the knowledge of the silicon 2p ionization limit and the $K\alpha$ emission energy (for SiF_4 and $SiCl_4$, see Ref. 1). The Si 1s ionization limit on $SiBr_4$ has been determined by the same method, i.e., in adding the Si 2p binding energy in this molecule as extracted from photoelectron spectroscopy[14] plus the atomic $K\alpha$ emission line.[15] Therefore, for $SiBr_4$, we obtain 1949.7 eV. We have estimated that the accuracy of the Si 1s ionization energies is ±0.7 eV. We have reported in Table I, the energies, term values, and relative intensities of each resonance observed in Figs. 1 and 2 plus those for deuterated silane. The SiD_4 spectrum is shown separately, in Fig. 3 together with part of the SiH_4 one, in order to see in more detail the numerous features found in the continuum, with a suitable enlargement.

In the first place, we observe that the SiH_4 and SiF_4 spectra show two intense lines in the discrete region, labeled 2 and 3 in Figs. 1(a) and 1(b), in contrast to those of $SiCl_4$ and $SiBr_4$ which show a unique intense line [labeled 2 in Figs. 1(c) and 1(d)] below the ionization edge. This point, which has been discussed in SiF_4 and $SiCl_4$ in our earlier publication[1] in terms of a Jahn-Teller effect, is reconsidered here with the comparison with the presented theoretical calculations and discussed below.

Secondly, the small but significant feature (1 in the SiF_4 spectrum of Fig. 1), already reported in our earlier publication,[1] has a counterpart in the other molecular case, except in silane. This is somewhat surprising since a similar feature has been observed in methane by Hitchcock, Pocock, and Brion.[16] Furthermore, the absence of any isotope effect in silane as evidenced by the identity between

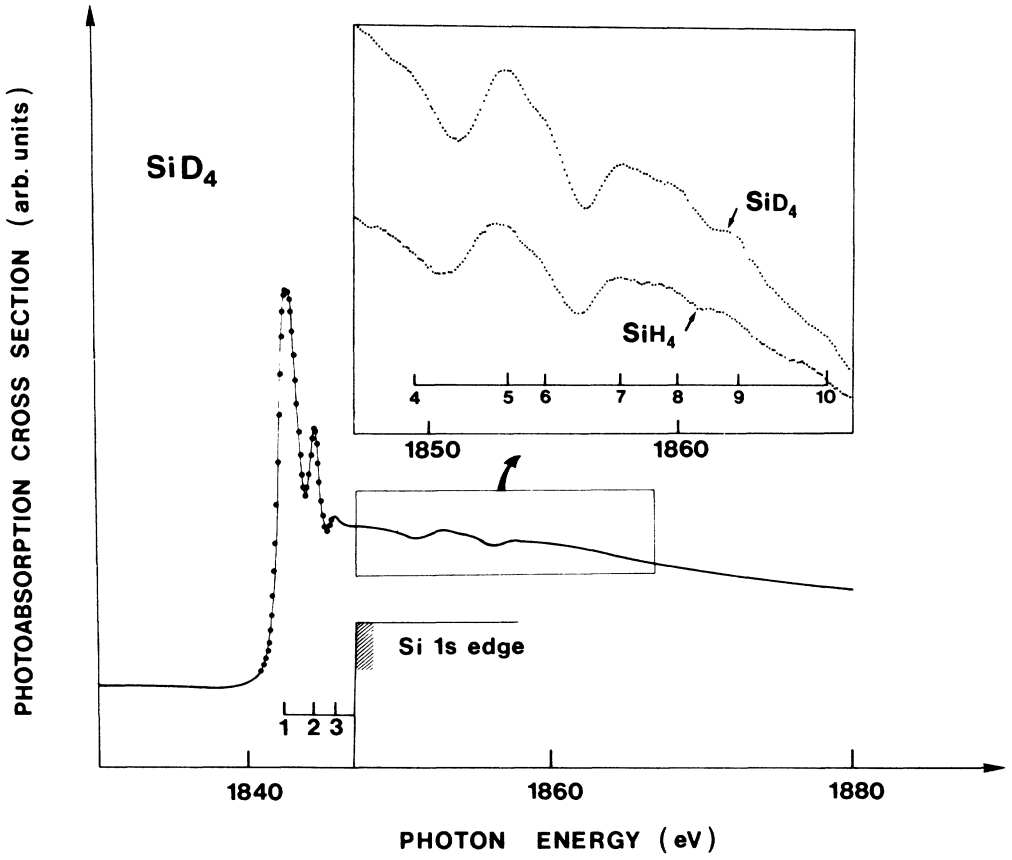

FIG. 3. Photoabsorption spectra of SiD_4 and SiH_4 with details of the double core-valence vacancy states.

SiD_4 and SiH_4 spectra contrasts with the methane case, for which a significant change in the intensity of this particular feature varies from CH_4 to CD_4. In $SiCl_4$ and $SiBr_4$, one observes an asymmetry or a shoulder rather than a resolved line. Nevertheless, we will analyze this point below, in terms of symmetry-forbidden transitions.

Thirdly, in Fig. 3 we observe several features found in the ionization continuum of the silane spectrum (Fig. 3) which have never been reported before. Despite the fact that we do not resolve all lines, we can safely consider that we are seeing numerous congested lines with a width smaller than 2 eV. The quasiabsence of the isotope effect for the line position and intensity is remarkable and shows readily that we deal with many electronic transitions. Their relative position with respect to the main resonance as well as their relatively small intensity favors immediately an interpretation in terms of double excitation transitions. This point will be discussed below.

Fourthly, by comparing the continuum features of the $SiCl_4$ and $SiBr_4$ spectra of Figs. 1 and 2, we have classified the narrow ones [labeled 3, 4, and 5 in Figs. 1(c) and 1(d)] from the wide ones [labeled 6 and 7 in Figs. 2(c) and 2(d)]. The first set has a typical full width at half maximum ranging from 1.9 to 2.3 eV, the width of the other extends to more than 10 eV. In addition, the narrow ones are found very close to the ionization threshold, at much lower energy than in the silane case. In contrast, the wide resonances are observed much further away in the continuum. The interpretation of these features in terms of multiple excitation effects and shape resonances will be discussed, as well as their counterpart in the SiF_4 molecule.

TABLE II. Experimental energies, term values, and suggested assignment of near-edge resonance in SiX_4 (X=CH_3,OCH_3,C_2H_5,OC_2H_5).

Peak	Photoionization Energies (eV)	Photoionization E_{TV} (eV)	Photoabsorption E_{TV} (Ref. 1)	Assignment
		$Si(CH_3)_4$		
1	1843.6	2.5	2.2	t_2
IP	1846.1	0	0	
2 (shoulder)	1848.2	−2.1		doubly excited
3	1853.9	−7.8	−8.2	shape
4	1906.0	−60.0		EXAFS
		$Si(C_2H_5)_4$		
1	1843.4	2.6		t_2
IP	1846.0	0		
2 (shoulder)	1849.9	−3.9		doubly excited
3	1854.5	−8.5		shape
4	1903.0	−57.0		EXAFS
		$Si(OCH_3)_4$		
1	1847.1	1.0		t_2
IP	1848.1	0		
2	1861.0	−12.9		shape
3	1925.0	−76.9		EXAFS
		$Si(OC_2H_5)_4$		
1	1846.9	1.1		t_2
IP	1848.0	0		
2	1861.5	−13.5		shape
3	1925.0	−77.0		EXAFS

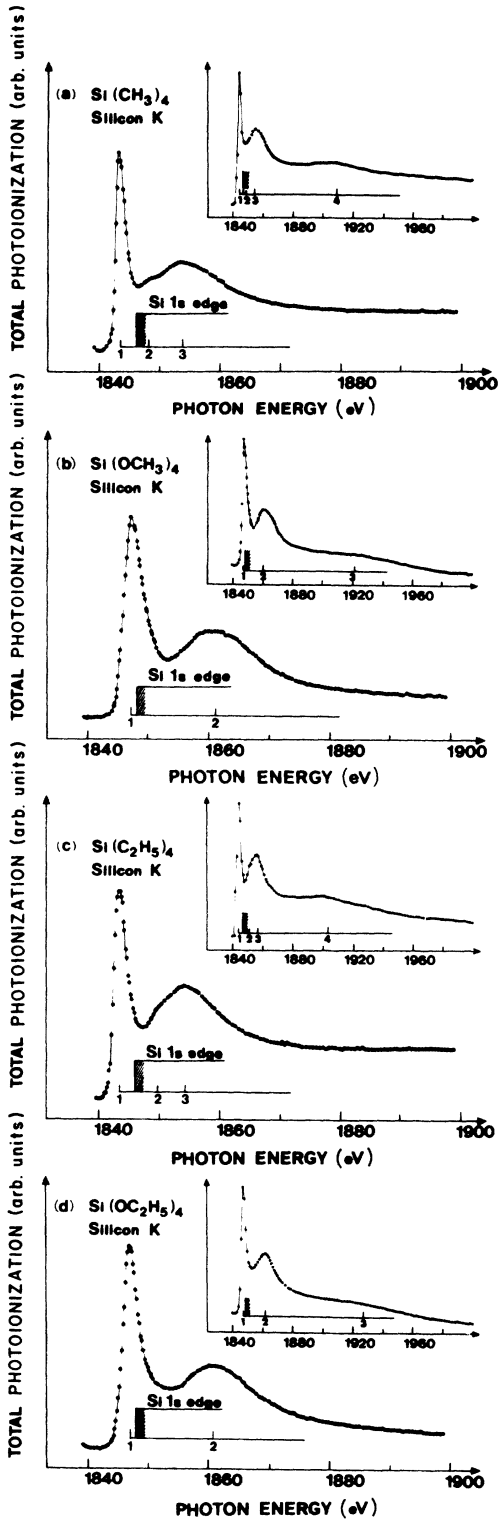

FIG. 4. Total photoionization spectra of SiX_4 (X=CH_3,OCH_3,C_2H_5,OC_2H_5) in the 1840–2000-eV photon energy range.

We present in Fig. 4 the total ionization spectra of SiX_4 (X=CH_3,OCH_3,C_2H_5,OC_2H_5) in the 1840–2000-eV photon energy range. Except for tetramethylsilane, for which the photoabsorption spectrum has been reported earlier,[1] all spectra are reported here for what we believe to be the first time. The presentation of the $Si(CH_3)_4$ spectrum is made because we observe a new feature (labeled 2 in Fig. 3), as compared to our previous article. We have also reported in the figure the Si 1s ionization limits. For X=CH_3 and OCH_3 we have used the same procedure as explained above. To determine them for X=C_2H_5 and OC_2H_5, we have assumed that the substitution of the methyl groups by ethyl ones does not change the core-ionization limit. We have reported in Table II the energies and term values of the various resonances seen in SiX_4 (X=CH_3,$OCH_3C_2H_5$,OC_2H_5).

The main trends of the spectra are the following. (i) There is a unique intense transition in the discrete part of the spectra and a well-pronounced resonance in the continuum for the whole series. (ii) The substitution of the methyl group by an ethyl group does not change the shape of the near-edge spectrum, except for a slight shift in energy of the resonances and a small variation of the position and intensity of the continuum features, with respect to the main discrete resonance. However, the presence of an oxygen atom rather than a carbon atom in the immediate vicinity of the silicon atom induces much larger changes on the resonance positions and widths. (iii) There is a pronounced assymmetry on the high-energy side of this main resonance, for X=OCH_3 and OC_2H_5, which does not exist for X=CH_3 or C_2H_5. For the latter, there is a significant shoulder on the low-energy side of the main continuum resonance [labeled 2 in Figs. 4(a) and 4(c)].

III. THEORETICAL

In the following we have calculated the term values of core-to-valence and core-to-Rydberg excited states in the series SiX_4 (X=H,F,Cl,Br). In other words, we have analyzed only "one-electron" core excited states found in the discrete part of the spectrum. For the one-electron part in the continuum, i.e., shape resonance and extended x-ray absorption fine-structure (EXAFS) oscillations, we only rely on the literature.[3,17] More calculations on this point will be published elsewhere.[18] Finally, no attempt was made to calculate multiple excitation states.

A. Method

We have performed all calculations using the approximation of the core-equivalent model. In principle, this approach is the most valid when the core vacancy is close to the nucleus, i.e., further away from the valence orbitals, and is therefore quite appropriate to the 1s core vacancy as in the present case. We have restricted the calculations to the silicon atom and then considered phosphorous as the core-equivalent species. The lowest core-excited state corresponds to the ground-state PX_4 molecule. Higher core-excited states correspond to excited (valence or Rydberg) species and the ionization limit to the PX_4^+ ion.

In the following we describe a simple and direct method for evaluating term values, including configuration interaction, very much like in the previous work of Friedrich *et al.* (for example, Ref. 19). Each term value corresponding to a given $1s \rightarrow i^*$ excitation (i^* valence or Rydberg) is taken as the energy difference between the suitable PX_4 state and the self-consistent-field (SCF) energy of the closed-shell PX_4^+ ion. In taking the SCF energy of the PX_4^+ ion for the zeroth-order wave function, we find that the term value T_i is equal to $-\varepsilon_i^* + \mathcal{P} + \mathcal{C}$, where ϵ_i^* is the SCF energy of the empty orbital, $\mathcal{P}$ is the repolarization term pictured in Fig. 5, as due to the presence of an extra electron in the i^* orbital, and $\mathcal{C}$ is the difference of the valence correlation term between the PX_4 and PX_4^+ states. For the PX_4^* calculations, we have used *ab initio* pseudopotentials[20] for the core electrons of phosphorus and ligand (F, Cl, Br) atoms. Gaussian basis sets are chosen to be triple ζ with polarization on phosphorous and double ζ on the X atom. Three s, three p, and three d diffuse orbitals centered on P allow us to describe the first Rydberg states. In the first place, we consider that it is reasonable to assume that the $\mathcal{C}$ term is negligible. Secondly, the repolarization term $\mathcal{P}$ is certainly important to consider. Notice that neglecting this term reduces the term value to $-\epsilon_i^*$ as obtained from the SCF calculation of the ion, and so we are within the Koopman's theorem approximation. Therefore, in order to take into account the valence electron repolarization effect, one needs to perform the configuration interaction in the monoexcited space. This is schematically pictured in Fig. 5. In addition, it is necessary to take into account accidental degeneracies as shown in Fig. 5(c). Then, one introduces diexcited configurations in which a single valence electron of PX_4^+ is excited. Notice that the latter are monoexcited configurations of (PX_4^* and one electron in the j^* orbital). Consequently, in order to obtain the first n core-excited states, the configuration interaction must be performed in the monoexcited configuration space with respect to each zeroth-order

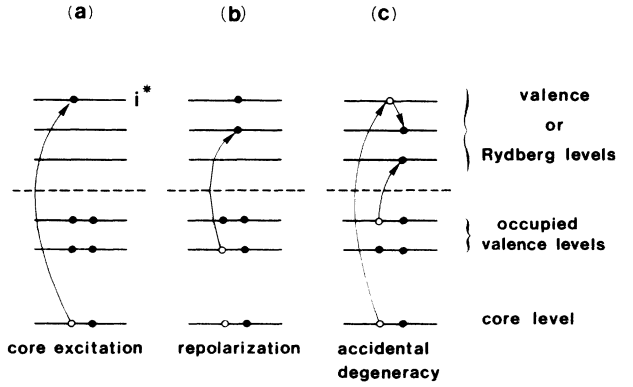

FIG. 5. Relevant mono and diexcitation configurations due to repolarization and accidental degeneracy.

configuration (with a total number n).

The transition intensities have been simply calculated by the dipole matrix element $\langle 1s|r|i^* \rangle$ in taking the $1s$ orbital of the silicon atom. This is because each i state after configuration interaction has a large weight on the zeroth-order configuration.

B. Tests

The first task is to ensure that the chosen configuration-interaction space takes into account the effects described above.

(i) For Rydberg states, for which the PX_4^+ relaxation is small, the term values must be close to those obtained by the Koopman's theorem. We show in Table III, in the SiF_4 case, that this difference is very small (<0.1 eV) for high Rydberg states in contrast to valence states for which gaps of 0.5 to 1 eV are found.

(ii) The valence electron correlation energy of PX_4^+ and of the different PX_4 excited states is assumed to be equal. Indeed, configuration of PX_4 with two excited valence electrons has not been included. It is certain that this assumption is fully valid for Rydberg states. Notice that for the present species, which do not have low-lying empty orbitals (such as π orbitals, Ref. 21), this is also true: We compare our results in Table IV for SiH_4, with previous calculations which do not use the core-equivalent approximation and do include such valence correlation effects.[22] The energy difference never exceeds 0.25 eV and is even much smaller for Rydberg states. Lastly, one can compare our results with $X\alpha$ calculations[23] available for SiF_4, as seen in Table III. We find in column 3 that the term values for valence states calculated in Ref. 18 are not as good as those found by our method, as compared to experimental results (see Sec. IV).

C. Results

We have reported in Table V the term values and intensities of valence and Rydberg transitions in SiX_4 (X=H,F,Cl,Br). They are also reported in Fig. 1. The most remarkable phenomenon is the collapse of the $1s \rightarrow 4p$ transition in going from SiF_4 to $SiCl_4$ and $SiBr_4$. This originates from the fact that the $4p$ orbital penetrates the core more deeply in SiF_4 than for other molecules. This is especially evident in the plot of Fig. 6, which shows the t_2^* and $4p$ wave functions along the Si-X coordinate, for both the SiF_4 and $SiCl_4$ molecules. The similarities of the pure valence orbital and the $4p$ show that the latter has a strong valence character. This is not the case for the $SiCl_4$ molecule for which the valence-

TABLE III. Comparison of term values (eV) of SiF_4 resonances, calculated at various levels of approximations.

Unoccupied level	$-\varepsilon_i^*$ (SCF) this work	E_{CI} this work	$E_{X\alpha}$ Ref. 23
a_1^*	4.97	6.14	7.0
t_2^*	2.64	3.30	5.3
$4s$	2.22	2.47	2.6
$4p$	1.61	1.92	2.1
$3d_e$	1.43	1.44	1.6
$3d_{t_2}$	1.41	1.43	
$5s$	1.14	1.22	1.6
$5p$	0.95	1.02	

TABLE IV. Comparison of term values (eV) of SiH_4 resonances, calculated at various levels of approximations.

Unoccupied orbital	$-\varepsilon_i^*$ this work	E_{CI} on PH_4 this work	E_{CI} on Si^*H_4 Ref. 22
a_1^*	3.61	3.91	4.04
t_2^*	2.72	3.09	2.85
$4p$	2.17	2.29	2.14
$5s$	1.58	1.65	1.63
$3d_e$	1.51	1.53	1.56

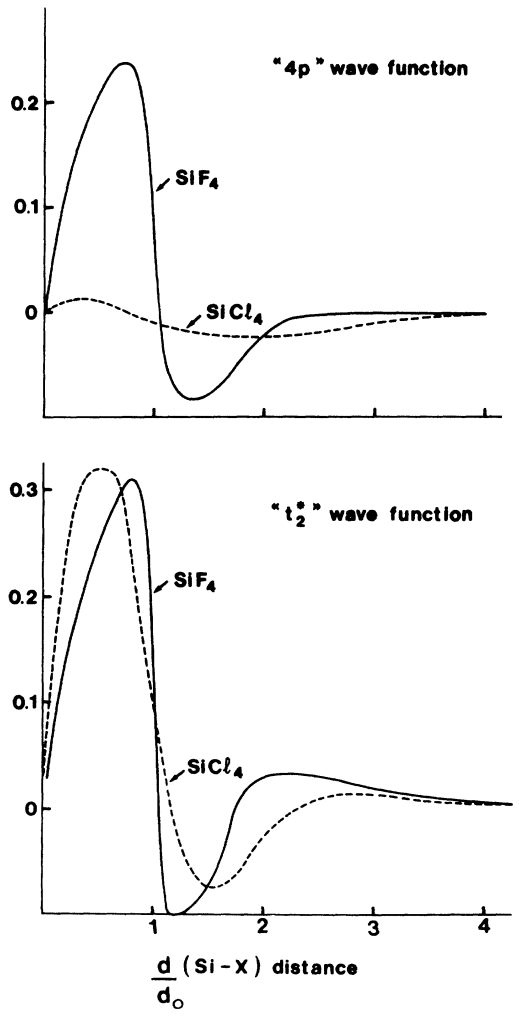

FIG. 6. Comparison of radial wave functions for the $4p$ orbital, in SiF_4 and $SiCl_4$. d_0 corresponds to the equilibrium interatomic distance in the ground-state molecule.

TABLE V. Calculated (Hartree-Fock and CI) term values, in eV, and relative intensities of discrete resonances in SiX_4 (X=H,F,Cl,Br). The asterisk denotes a normalized value.

	E_{TV}				E_{TV}		
	HF	CI	I		HF	CI	I
	SiH_4				SiF_4		
a_1	3.61	3.91		a_1	4.97	6.14	
t_2	2.72	3.09	1*	t_2	2.64	3.30	1*
$4s$				$4s$	2.22	2.47	
$4p$	2.17	2.29	1.03	$4p$	1.61	1.92	1.18
$5s$	1.58	1.65		$3d_e$	1.43	1.44	
$3d_e$	1.51	1.53		$3d_{t_2}$	1.41	1.43	
$3d_{t_2}$	1.20	1.24	0.0069	$5s$	1.14	1.22	
$3d_{t_2}$	1.09	1.12	0.34	$5p$	0.95	1.02	0.34
	$SiCl_4$				$SiBr_4$		
a_1	5.25	6.73		a_1	5.25	6.60	
t_2	3.04	4.60	1*	t_2	3.06	4.60	1*
$4s$	2.31	2.48		$4s$	2.31	2.49	
$4p$	1.81	1.90	0.015	$4p$	1.73	1.83	0.0049
$3d_e$	1.33	1.35		$3d_e$	1.28	1.31	
$3d_{t_2}$	1.28	1.34		$3d_{t_2}$	1.24	1.30	
$5s$	1.21	1.26		$5s$	1.16	1.22	
$5p$	0.92	0.98	0.0045	$5p$	0.92	0.94	0.0013

Rydberg mixing is very small. More details of such valence-Rydberg mixing can be found in Table VI. Further comparison with the present experimental results will be made in Sec. IV.

IV. DISCUSSION

A. Valence and Rydberg transitions

The first point of this discussion is to assign discrete resonances by taking advantage of the present theoretical calculations. The comparison between theory and experiment for the line position and relative intensity can be appreciated from Fig. 1 and Tables I and V. The agreement is satisfactory for X=F,Cl,Br but not for silane. In this case, a difference of 1.4 eV is found. This gap is slightly larger than our total experimental error bar if we include the absolute energy calibration (±0.5 eV) and the uncertainty of the Si $1s$ ionization limit (±0.7 eV). This discrepancy is also found with previous calculations[21] and is not understood at this time. Nevertheless, we can safely assign the most intense transition in the discrete spectrum as an electric dipole-allowed transition Si $1s \rightarrow \sigma^*(t_2)$ in which $\sigma^*(t_2)$ represents one of the valence antibonding Si-X orbitals. The other possible transition Si $1s \rightarrow \sigma^*(a_1)$ is symmetry forbidden in the tetrahedral symmetry group. The significant intensity found for this core-excited state is discussed below.

TABLE VI. Molecular-orbital coefficients on Gaussian basis functions centered on the silicon atom. V, I, and R refer to valence, intermediate, and Rydberg, respectively.

Basis	SiF_4		$SiCl_4$	
exponent	t_2^*	$4p$	t_2^*	$4p$
0.42 (V)	0.248	−0.280	0.327	−0.039
0.15 (V)	0.506	−0.558	1.059	−0.159
0.055 (I)	0.162	−0.197	0.148	−0.077
0.020 (R)	0.603	0.058	−0.024	0.437
0.0075 (R)	−0.073	0.792	0.101	0.706
0.0028 (R)	−0.004	0.014	−0.031	−0.018

The most important finding of the present calculation is that one expects the Si $1s \rightarrow 4p$ transition to be intense in both SiH_4 and SiF_4, but not for $SiCl_4$ or $SiBr_4$ because of the valence-Rydberg mixing of the t_2^* and $4p$ orbitals, which are strong for the first set of molecules and not for the second. Notice that multiple-scattering $X\alpha$ calculations[3] in $SiCl_4$ give the lowest Rydberg state, around 2 eV above the main valence transition, in agreement with the present CI calculations. However, there is a large discrepancy for its relative intensity (a factor of 10 higher in Ref. 3). If this intensity is correct, this Rydberg state should be observed experimentally. On the other hand, if this state is responsible for structure 3 in Fig. 1(c), as stated in Ref. 3, the calculated term value is off by 3 eV. Consequently, we consider that structure 3 has another interpretation (see Sec. IV B). We wish now to rationalize this valence-Rydberg mixing in considering the following arguments.

The Rydberg orbitals centered on the silicon atom must be orthogonal to molecular valence orbitals, including the lone pair orbitals found on the ligands. Consequently, the corresponding wave function presents a node at the center of the ligand atoms (see Fig. 6). The condition to find such a node is to combine the silicon orbitals together. Only those orbitals for which the amplitude is significant at this distance must be considered. For small Si-X interatomic separations, the amplitude of valence orbitals is rather large and they participate in the mixing. For large interatomic separations, such an amplitude vanishes and only Rydberg orbitals are combined. Having in mind that the large oscillator strength originates from the $\langle \text{Si } 1s|r|v^* \rangle^2$ component of the overall matrix

TABLE VII. Silicon-ligand distances on SiX_4 molecules. Values in parentheses denote the last uncertain digit.

Molecule	Si-X distance (Å)
SiH_4	1.481(1)
SiF_4	1.554(4)
$Si(OCH_3)_4$	1.64
$Si(CH_3)_4$	1.875(2)
$SiCl_4$	2.019(4)
$SiBr_4$	2.17

element, with v^* being a localized unoccupied orbital (as opposed to a diffused orbital), we expect that only transitions of Si $1s$ to Rydberg orbitals with mixed valence character will show up in the core-excited spectrum. We have reported in Table VII the Si-X distances for the present molecules, as extracted from literature. We clearly see that SiH_4 and SiF_4 occupy a special situation compared to the other molecules. The absence of any Rydberg-like peak in $Si(CH_3)_4$ or $Si(C_2H_5)_4$ can be explained by the rather large Si-X separation. The case of $SI(OCH_3)_4$ and $Si(OC_2H_5)_4$ is somewhat different. The main peak is located close to threshold. In other words, the corresponding term value is small. In addition it is tempting to assign the pronounced assymmetry on the high-energy side of this main peak in considering a Rydberg transition with a mixed valence character, because these two molecules have an intermediate Si-X distance compared to X=F and X=CH_3. However, we do not favor this interpretation because one expects that doubly excited states, as for the rest of the series, may be very close to threshold. This point is discussed below.

The importance of valence-Rydberg mixing, in particular in the SiF_4 molecule, makes out early interpretation of resonances 2 and 3, (Ref. 1) using the Jahn-Teller interaction obsolete. Let us reconsider such an effect in the general framework of vibronic coupling effects. In the first place, we reject possible electric quadrupole transitions in the present case of photon impact because such effects expected in electron-impact experiments have been found negligible in the electron energy loss of methane excited with 2.5-keV incident energy.[16] We believe then, within the electric dipole transition framework, that vibronic effects may bring intensity to symmetry-forbidden excited states. Consequently, we interpret the weak peak labeled 1 in Figs. 1(b), 1(c), and 1(d) as due to the Si $1s\rightarrow\sigma^*(a_1)$ transition, in accord with our previous assignment. The origin of such a vibronic coupling effect is because the core-excited state is more stable in the distorted geometry than in the tetrahedral one and because specific vibrational modes are activated. In order to confirm this point in the SiF_4 case, we have evaluated the relative energy of the core-equivalent PF_4 molecule in two equilibrium geometries, i.e., a tetrahedral and a trigonal bipyramid.[1] We have found that the lowest state A_1 [Si $1s\rightarrow\sigma^*(a_1)$] has a distorted geometry rather than a tetrahedral one with a 2-eV gap. We have also evaluated that this gap decreases to 0.2 eV for the T_2 state [Si $1s\rightarrow\sigma^*(t_2)$]. Consequently, the significant intensity for the Si $1s\rightarrow\sigma^*(a_1)$ transition [Figs. 1(b), 1(c), and 1(d)] is likely due to high asymmetric vibrational levels. However, for $\sigma^*(t_2)$ transitions, for which such vibronic coupling becomes a static Jahn-Teller effect, one should expect a removal of the degeneracy of about a fraction of an eV. But this is much smaller than the lifetime broadening (0.5 eV) and should not induce any observable effect on the spectrum. Finally, notice that the absence of the $\sigma^*(a_1)$ transition in silane puts this molecule in a specific situation, compared to the series X=F, Cl, Br and to the methane carbon $1s$ spectrum.[16] The same situation is found for the molecules of Fig. 4.

B. Double core-valence vacancy-excited states

In a recent paper,[12] we have shown that for most of the present series of molecules we observe double core vacancy-excited states resulting from the simultaneous excitation of a Si $1s$ and a Si $2p$ electron into an unoccupied valence orbital, i.e., Si $1s\rightarrow v^*$, Si $2p\rightarrow v^*$. The observed structures are found as a multiplet with a relative intensity of less than 1% of the main core-to-valence transition. Having in mind that the valence-to-valence unoccupied (v^*) transitions have a much larger oscillator strength than the Si $2p$ to v^*, it is reasonable to consider double core-valence vacancy-excited states, i.e., Si $1s\rightarrow v^*$, $v\rightarrow v^*$ with a much larger relative intensity than for the double core vacancy-excited states.

The most clear-cut case in the present series is the silane molecule, as seen in Fig. 3, because we do not expect any significant shape resonance because the hydrogen atom is a poor backscatterer. The weak and numerous structures in the immediate vicinity above the ionization edge appear from 7 to 24 eV above the main Si $1s\rightarrow\sigma(t_2)^*$ peak, and are certainly due to multiple excitation. Similar findings have been made in the isoelectronic species like argon near the $1s$ edge[24] and H_2S near the S $1s$ edge.[25] We offer to consider double excitation features of the following type:

$$\text{Si } 1s^{-1}v^{-1}\rightarrow(v^*)^2 ,$$

with v being one of the Si-H σ-bonding orbitals, a_1 or t_2, and with v^* being one of the unoccupied valence orbitals t_2^* and $4p$ discussed above. At higher energy we should consider several features due to excitation plus ionization converging to the double ionization onset Si $1s^{-1}v^{-1}$, i.e.,

$$\text{Si } 1s^{-1}v^{-1}\rightarrow v^*,\epsilon k .$$

Let us analyze qualitatively the energy position of such doubly excited states. Following our previous calculations on double core vacancy states in these molecules,[12] we find that

$$E_{cv\rightarrow v^*v^*}=E_{c\rightarrow v^*}+E_{v\rightarrow v^*}+\mathcal{J}+\mathcal{K}+\mathcal{C} ,$$

where $E_{c\rightarrow v^*}$ and $E_{v\rightarrow v^*}$ are the single core and valence excitation energies, $\mathcal{J}$ is the total Coulomb interaction term with $\mathcal{J}=J_{cv}+J_{v^*v^*}-J_{cv^*}-J_{vv^*}$, $\mathcal{K}$ is the exchange term, and $\mathcal{C}$ is the electronic correlation term. We know that in silane the first valence transition $E_{v\rightarrow\sigma^*}$ amounts to 9 eV.[26] It is reasonable to consider that the $\mathcal{J}$ and $\mathcal{K}$ terms amount to several eV, either with a positive or neg-

ative sign. Consequently, the structures labeled 4 to 6 in Fig. 3 and, respectively, located at 7, 10.4, and 12 eV with respect to the main transition $\sigma^*(t_2)$ are compatible with this interpretation. Higher features labeled 7 to 10 are also compatible, having in mind that there are two v^* and two v orbitals with a_1 and t_2 symmetry (separated, respectively, by 1.7 eV as seen in Table I and 6 eV as extracted from photoelectron spectra[27] which can be involved. This increases largely the final density of states compared to the double core vacancy case.[12] As a result, it is very difficult to give a more precise assignment without calculations.

Let us consider the other molecules. Since the silane molecule shows multielectron effects, it is reasonable to expect them in the rest of the series. However, lone-pair electrons of the halogen ligands must play a great role and the higher number of valence electrons leads to an increase in intensity of the corresponding structures. The most clear case is the $SiCl_4$ molecule, as seen from Figs. 1(c) and 2(c). Our main argument is based on the large difference in the width of doubly excited features as compared to shape resonances. Shape resonances are well known to be described using a potential barrier model which is a pure "one-electron" approach. In other words, the main decay channel of such resonance is unique, i.e., the ejection of the core electron in the continuum. This is a fast process and as a result, their widths are of the order of 5 to 10 eV (Refs. 28 and 29) except in very specific cases such as SF_6 near the S $2p$ edge[30,31] and SiF_4 near the Si $2p$ edge.[19,32] In contrast, doubly excited states generally require an autoionization description because their decay channels are many, and two (or more) electrons are generally involved. Detailed photoelectron spectroscopy work such as the recent study on the SF_6 molecule near the S $2p$ edge by Ferrett *et al.*[31] would be necessary to confirm this analysis. Nevertheless, it is expected that their widths are generally much smaller, i.e., at most 1 or 2 eV typically.[28,31] In $SiCl_4$, the features labeled 3 to 5 seen in Fig. 1(c) are much narrower (width of around 2 eV) compared to features 6 and 7 in Fig. 2(c) (width of 12 and 20 eV). On the other hand, we must expect double excited states in a rather extended energy range as seen for the silane case. Then we believe that the features labeled 3 to 5 are likely doubly excited states. This interpretation is compatible with the photoabsorption spectrum of this molecule near the Si $2p$ edge.[2,33] There is a strong multiplet feature which lies only some 6 eV above the lowest transition Si $2p \rightarrow \sigma^*$ and is positioned right on top of the ionization edge, with a multiplet shape extending over 4 eV. Since we do not have to consider Rydberg transitions, this feature may well be the counterpart of the present observations. Notice that, in $SiCl_4$, the alternative interpretation given by Tse *et al.*[3] about the strong structure near threshold in the Si $2p$ spectrum,[2] is not convincing, since both the term value and relative intensity do not agree at all with experiment. If the present interpretation is correct then one finds such doubly excited states at much lower energy compared to the silane case. We believe then that there is a stabilization of such double excited states by a charge transfer from the lone pairs of the chlorine ligands onto the silicon atom, with the effect of screening of the positive charge. In other words, this would mean a strong configuration interaction between the two following sets of states:

$$\text{Si } 1s^{-1} \rightarrow v^*, v(\text{Si-}X) \rightarrow v^* ,$$

$$\text{Si } 1s^{-1} \rightarrow v^*, v(\text{lone pair}) \rightarrow v^* .$$

Similar situations have been calculated by Schirmer, Barth, and Tarantelli[34] in the C $1s$ photoabsorption spectrum of formaldehyde, for which a double core-valence excited state C $1s,O(n) \rightarrow (\pi^*)^2$ is found only 2.3 eV above the main C $1s \rightarrow \pi^*$ transition. Another example is the C $1s$ photoabsorption spectrum of benzene, which presents a very low-lying doubly excited state as interpreted by Schwarz *et al.*[35]

Now the question is how to assign shape resonances. Let us consider in detail features labeled 4, 5, and 6 in Figs. 1(c) and 2(c) for $SiCl_4$. In restricting the argument to the width, the feature labeled 6 which lies some 25 eV above the ionization limit is certainly a good candidate for a shape resonance. Indeed, Carlson *et al.*,[17] as well as Tse *et al.*[3] calculated two shape resonances in the Si $2s$ continuum at 10 and 20 eV above the edge. Other preliminary calculations also find the same results.[36] Now the question is to assign the structures 4 and 5 which lie, respectively, at 7.1 and 9.9 eV. The latter lies exactly at the predicted position of a shape resonance. However, its width is not compatible with a one-electron feature. As seen above, one expects a large number of multiplets because there are different (Si $1s^{-1}v^{-1}, v^*v^{1*}$) configurations, each of them leading to different states with a variety of multiplet splittings. It is then reasonable to expect that the apparent width of features 4 and 5 is due to the congestion of these states. In this case the amplitude of the underlying shape resonance would be too weak to emerge from the continuum. Although we favor this latter interpretation, more work is needed both on the theoretical and experimental (photoelectron spectroscopy) side to clarify this point.

The similarities between the $SiCl_4$ and $SiBr_4$ spectra are very strong (Fig. 1). It is reasonable to consider, even without knowing the Si $2p$ photoabsorption spectrum, that the features labeled 3 to 5 are also doubly excited states, in which the bromine lone pairs are screening somewhat the Si $1s$ core hole. Notice that the amplitude of feature 7 is very weak in $SiBr_4$ compared to those of $SiCl_4$. This behavior is in good agreement with calculations of backscattering amplitude[37] which predict a much lower value for bromine than chlorine in the energy range considered here.

The SiF_4 case is now more puzzling. There are two features, labeled 4 and 5, in the immediate region above the edge. In our previous paper, we have tentatively assigned them as shape resonances in the t_2^* partial ionization continuum. Although feature 5 has a width compatible with a shape resonance, we propose that the shoulder labeled 4 in Fig. 1(b) is likely to be a doubly excited state merging into the shape resonance. If it is so, the fluorinated molecule would be very different from the chlorinated or brominated species, for which there is no

clear evidence of an overlap. Notice that no calculations have been done for this molecule and a precise evaluation (energy and width) of any shape resonance in the continuum would be very helpful.

Let us consider now the molecules of Fig. 4. We note that the ligands of $Si(CH_3)_4$ or $Si(C_2H_5)_4$ do not have a lone pair and can be compared to the silane molecule. In contrast, for $X=OCH_3$ or $X=OC_2H_5$, the oxygen atom carries a lone pair which can also play the same role as the halogen ligands. We propose that for $X=CH_3$ and C_2H_5 the structure labeled 2 is a doubly excited state, with a possible superposition with a shape resonance (feature 3). We also propose for $X=OCH_3$ and OC_2H_5, that the high-energy tail of the main peak is due to the doubly excited states (rather than Rydberg states), since the first shape resonance has a nice symmetric shape.

V. CONCLUSION

We have observed in the photoabsorption spectra of gas-phase silicon compound molecules, with tetrahedral symmetry, many different types of resonances with a variety of widths, all of them varying in position and intensity with the nature of the ligands.

Below the ionization edge, we show, using the Hartree-Fock model applied to the core-equivalent molecule, that only core-excited states resulting from monoelectronic transitions to valence unoccupied orbitals are observed. Core-excited states resulting from transitions into Rydberg orbitals have a negligible oscillator strength, except for SiH_4 and SiF_4, for which the lowest Rydberg orbital $4p$ has a strong valence character. We suggest that the variation of the valence-Rydberg mixing is related to the Si-X interatomic distance.

Above the ionization edge, we show that double core-valence vacancy-excited states have a significant intensity extending over a complex multiplet structure. Except for silane, they are found at surprisingly low energy, probably because of the screening of the positive charge by the lone-pair electrons of the ligands. Complications on the assignment of specific multiplet components arise because of the existence of shape resonances in the same photon energy region. Calculations on both shape resonances and double core-valence vacancy-excited states are needed to confirm our present understanding of the first 20 eV in the continuum region of this series of molecules.

ACKNOWLEDGMENTS

We are grateful to A. P. Hitchcock for a critical reading of the manuscript, to E. Lizon à Lugrin for technical assistance, and to the Laboratoire pour l'Utilisation du Rayonnement Electromagnétique staff for operating the ACO storage ring and for general facilities. We are indebted to M. Cauchetier and M. Luce for help in preparing toxic samples, and to S. Tistchenko for preparing SiD_4 gas. The Laboratoire pour l'Utilisation du Rayonnement Electromagnétique is "Laboratoire mixte, Centre National de la Recherche Scientifique, Commissariat à l'Energie Atomique, et Ministère de l'Education Nationale."

[1]S. Bodeur, I. Nenner, and P. Millié, Phys. Rev. A **34**, 2986 (1986); **37**, 644(E) (1988).

[2]J. D. Bozek, K. H. Tan, G. M. Bancroft, and J. S. Tse, Chem. Phys. Lett. **138**, 33 (1987).

[3]J. S. Tse, Z. F. Liu, J. D. Bozek, and G. M. Bancroft, Phys. Rev. A **39**, 1791 (1989).

[4]S. Bodeur and I. Nenner, J. Phys. (Paris) Colloq. Suppl. 12, **47**, C8-79 (1986).

[5]M. Lemmonier, O. Collet, C. Depautex, J. M. Esteva, and D. Raoux, Nucl. Instrum. Methods **152**, 109 (1978).

[6]S. Bodeur and J. M. Esteva, Chem. Phys. **100**, 415 (1985).

[7]A. P. Hitchcock and M. Tronc, Chem. Phys. **121**, 265 (1988).

[8]F. W. Lytle, R. B. Gregor, G. H. Via, J. M. Brown, and G. Meitzner, J. Phys. (Paris) Colloq. **47**, C8-149 (1986).

[9]E. R. Austin and F. W. Lampe, J. Phys. Chem. **80**, 2811 (1976).

[10]L. G. Parrat, C. F. Hempstead, and J. L. Jossem, Phys. Rev. **105**, 1228 (1957).

[11]C. Senemaud (private communication).

[12]S. Bodeur, P. Millié, E. Lizon á Lugrin, I. Nenner, A. Filiponi, F. Boscherini, and S. Mobilio, Phys. Rev. A **39**, 5075 (1989).

[13]R. G. Cavell and R. N. S. Sodhi, J. Electron Spectrosc. Relat. Phenom. **15**, 145 (1979).

[14]A. A. Bakke, H. W. Chen, and W. L. Jolly, J. Electron Spectrosc. Relat. Phenom. **20**, 333 (1980).

[15]Y. Cauchois and C. Sennemaud, *Wavelengths of X-ray Emission Lines and Absorption Edges* (Pergamon, New York, 1978).

[16]A. P. Hitchcock, M. Pocock, and C. E. Brion, Chem. Phys. Lett. **49**, 125 (1977).

[17]T. A. Carlson, W. A. Swensson, M. O. Krause, T. A. Whitley, F. A. Grimm, G. Von Wald, J. W. Taylor, and B. P. Pullen, J. Chem. Phys. **84**, 122 (1986).

[18]M. Benfatto, C. R. Natoli, S. Bodeur, and I. Nenner (unpublished).

[19]H. Friedrich, B. Pittel, P. Rabe, W. H. E. Schwarz, and B. Sonntag, J. Phys. B **13**, 25 (1980).

[20]P. Durand and J. C. Barthelot, Theor. Chim. Acta **38**, 283 (1975).

[21]W. H. E. Schwarz, T. C. Chang, U. Seiger, and K. H. Hwang, Chem. Phys. **117**, 73 (1987).

[22]H. Friedrich, B. Sonntag, P. Rabe, W. Butscher, and W. H. E. Schwarz, Chem. Phys. Lett. **64**, 360 (1979).

[23]R. Szargan, M. Meisel, E. Hartmann, and G. Brunner, Jpn. J. Appl. Phys. Supp. 17-2, **17**, 174 (1978).

[24]R. D. Deslattes, R. E. Lavilla, P. L. Cowan, and A. Henins, Phys. Rev. A **27**, 923 (1983); J. W. Cooper, *ibid.* **38**, 3417 (1988).

[25]J. Hormes, U. Kuetgens, and I. Ruppert, J. Phys. (Paris) Colloq. Suppl. 12, **47**, C8-569 (1986).

[26]M. B. Robin, *Higher Excited States of Polyatomic Molecules* (Academic, London, 1985), Vol. III.

[27]G. G. B. de Souza, P. Morin, and I. Nenner, Phys. Rev. A **34**, 4770 (1986).

[28]P. Morin, I. Nenner, M. Y. Adam, M. J. Hubin-Franskin, J. Delwiche, H. Lefebvre-Brion, and A. Giusti-Suzor, Chem. Phys. Lett. **92**, 609 (1982).

[29]D. W. Lindle, C. M. Trusdale, P. H. Kobrin, T. A. Ferrett, P. H. Heimann, U. Becker, H. G. Kerkhoff, and D. A. Shirley, J. Chem. Phys. **81**, 5375 (1984).

[30]T. M. Zimkina and V. A. Fomichev, Dokl. Akad. Nauk. SSSR **169**, 1304 (1966) [Sov. Phys.—Dokl. **11**, 726 (1967)].

[31]T. A. Ferrett, D. W. Lindle, P. A. Heimann, M. N. Piancastelli, P. H. Kobrin, H. G. Kerkhoff, U. Becker, W. D. Brewer, and D. A. Shirley, J. Chem. Phys. **89**, 4726 (1988).

[32]G. G. B. de Souza, P. Morin, and I. Nenner, J. Chem. Phys. **90**, 7071 (1989).

[33]V. A. Fomichev, T. M. Zimkina, A. S. Vinogradov, and A. M. Evdokimov, Zh. Strukt. Khim. **11**, 676 (1970).

[34]J. Schirmer, A. Barth, and F. Tarantelli, Chem. Phys. **122**, 9 (1988).

[35]W. H. E. Schwarz, T. C. Chang, U. Seeger, and K. H. Hwang, Chem. Phys. **117**, 73 (1987).

[36]S. Bodeur, J. L. Ferrer, I. Nenner, P. Millie, M. Benfatto, and C. R. Natoli, J. Phys. (Paris) Colloq., Suppl. 12, **48**, C9-1117 (1987).

[37]B. K. Teo and P. A. Lee, J. Am. Chem. Soc. **101**, 2815 (1979).